

# Experimental Evaluation of The Ultimate Capacity of External RC Beam-Column Joints

A. Masi, G. Santarsiero & D. Nigro

University of Basilicata, Potenza, Italy



## SUMMARY:

Some results of a wide experimental program carried out on beam-column RC joints are presented. All the experimental tests were performed at the Laboratory of Structures of the University of Basilicata, Italy. Current assessment procedures on existing buildings usually neglect the variations of joint stiffness due to axial load variations. Main objective of the paper is to show how the axial load value on the columns can affect both ultimate capacity and stiffness of joints. To this purpose, the behaviour of three identical specimens tested under different axial load values is analysed and compared in terms of ultimate capacity and deformation behaviour. Results show significant variations of the joint stiffness at increasing drift values and, moreover, that the main source of deformability moves from the beam to the joint panel when the axial load decreases. The increase in joints' deformability is mainly due to early cracking of the joint panel as a consequence of the stress state determined by low axial load values.

*Keywords: Reinforced concrete, beam-column joint, secant stiffness, ultimate capacity, collapse mode*

## 1. INTRODUCTION

Design procedures of new buildings and assessment procedures of existing ones devote generally large attention to beam and column members paying less attention to the intersection region. However, under seismic actions the joint panel is subject to shear action several times higher than that of the framing members. This is due to both its aspect ratio and opposite sign of beam bending moments at opposite faces of the joint (Fardis, 2009). For this reason, the panel can suffer brittle failure and threaten the capacity of the entire structure, thus reducing the benefits of an effective design of beam and column members. Indeed, past earthquakes (e.g. Abruzzo 2009) have shown that joint performances have a very important influence on the strength and the overall stability of RC framed structures.

Frequently, experimental tests on beam-column joints concentrate on buildings designed to resist only gravity loads (Hakuto et al., 2000), because of their higher vulnerability and wide presence in many earthquake-prone countries. Main objective is to establish reliable methods for assessing resistance and deformability of joints and, as a consequence, to develop effective retrofit techniques.

Other investigations have been carried out on joints belonging to seismically designed structures with the objective of verifying the influence of some detail solutions on the behaviour and collapse mechanism. Among them, some studies have highlighted the influence of the anchorage type within the joint adopted for the longitudinal beam bars (Park, 2002; Calvi et al., 2002; Kusuhara & Shiohara, 2008).

The present paper focuses on the experimental evaluation of the effects of axial load on the seismic performances of beam-column joints. As a matter of fact, axial force has a large influence on the shear strength of the joint, as recognized in the capacity models given in the literature (e.g. Paulay & Priestley, 1992). Code-complying specimens have been investigated, namely specimens designed to match the rules given by the past Italian seismic code OPCM 3274, which are substantially consistent with the current Italian structural code (NTC08, 2008) and the EuroCode 8 (CEN, 2004b). Analysis of performance is carried out taking into consideration both ultimate capacity and deformation behaviour.

## 2. EXPERIMENTAL INVESTIGATION

The present paper is based on an experimental investigation carried out in the framework of the DPC-ReLUIIS research project funded by the Department of Civil Protection (DPC) and coordinated by the Italian Network of Earthquake Engineering Laboratories (ReLUIIS). Specifically, the study was included in the Research Line 2 devoted to the “Assessment and reduction of seismic vulnerability of existing RC buildings”. All the experimental activities described in the paper have been performed at the Laboratory of Structures of the University of Basilicata, Potenza, Italy.

Globally, the experimental program foresees cyclic loading tests on 26 beam-column joint specimens built in 2006. The experimental tests began some months later and 14 tests have been carried out up to date, 3 of them are specifically analysed in the present paper. A full description of the experimental program is reported in (Masi et al., 2012).

### 2.1 Test Specimens

The specimens are one-way external joints belonging to the first storey of an internal frame of a four storey RC building (prototype structure) designed to resist earthquake loads according to the seismic code OPCM 3274 (PCM, 2003) in effect in Italy when the specimens were designed. It is worth remembering that the provisions of OPCM 3274 concerning seismic design are substantially consistent with the current Italian structural code (NTC08, 2008) as well as with the Eurocode 8 (CEN, 2004b).

The three specimens described and analyzed in the following are designed to resist earthquake actions considering a medium seismicity zone (Zone 2,  $a_g = 0.25g$ ), where  $a_g$  is the design ground acceleration at the ultimate limit state (life safety).

The joints have beams with 300x500 mm cross section and columns with 300x300mm cross section. The reinforcement is made up of deformed bars of B450C class.

The three joints are identical from the geometric and the detailing point of view but have been tested under different values of the axial compression load acting on the column. They are, therefore, named “Jxx”, where “J” is for joint and “xx” is a number representing the axial load level as a percentage of the ultimate axial load: the specimen J5 has been tested applying an axial load equal to 5% of the ultimate value  $N_u = b h f_c$ , the specimen J15 has been tested under an axial load equal to 15% of  $N_u$  and, finally, the specimen J30 under an axial load equal to 30% of  $N_u$ .  $b$  and  $h$  are the column cross section dimensions and  $f_c$  is the mean cylinder compression strength of the concrete. In Fig. 1 the reinforcement detailing arranged in the joints is displayed.

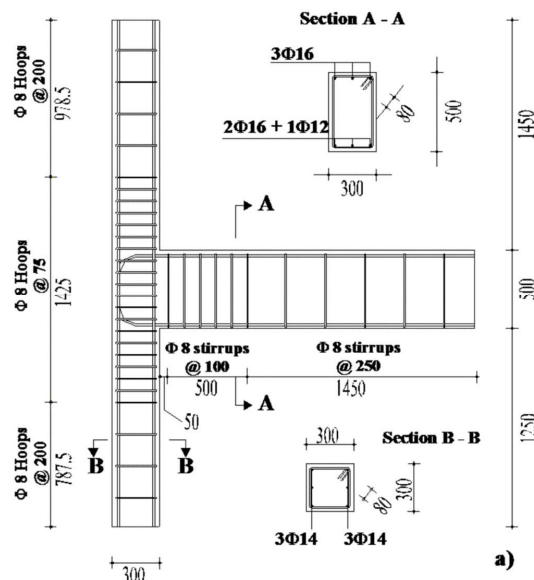


Figure 1. Detailing of the joint specimens

In the design procedure of the prototype structure a soil type A (rock or other rock-like geological formation) was considered, assuming a behaviour factor  $q$  equal to 4.095 coherently with the adopted code provisions for the structural type under analysis, and following the code requirements related to a low ductility class (CD B). It is worth specifying that low ductility RC structures do not have to explicitly follow capacity design rules, but only adopt prescribed reinforcement details and minimum amounts of steel, thus implicitly providing appropriate values of the members' local ductility.

The reinforcement cage was built by workers usually employed in the construction of RC building structures. Therefore, no special attention was paid in constructing the specimens, so that they can have the typical defects of real structures.

Differently from other experimental investigations, where concrete casting was made by putting the formwork on a horizontal plane (e.g. Braga et al., 2001), specimens were made by vertical casting. In such a way, differences in concrete strength along the height of the columns can occur because of the segregation effects of the aggregates and capillary rise of water, as typically found in real structures.

Before the execution of the cyclic tests on the joints, also the constituent materials were tested to obtain their mechanical properties.

At the beginning of the experimental program, some concrete cubes were subjected to compression tests in order to estimate their strength, achieving a mean value equal to  $f_c=21.5$  MPa. Further tests were performed during the program showing that concrete strength remained practically constant.

In order to determine the main mechanical properties of steel, some bars were subjected to tensile tests providing results in terms of yielding strength  $f_y$ , tensile strength  $f_t$ , and ultimate strain  $\epsilon_u$ . Test results were consistent with the type of steel used, i.e. B450C, in line with the current Italian structural code (NTC08, 2008) and corresponding to hot rolled steel of class C according to Eurocode 2 (CEN, 2004a). The mean value of the yielding strength was equal to  $f_y=480$  MPa, while the ultimate strain was equal to  $\epsilon_u=11.4\%$ .

## 2.2. Test Set-up

Different arrangements of the test set-up are used in the experimental investigations reported in literature (e.g. Hwang et al., 2004), where the acting force is applied either to the column or to the beam.

The tests carried out in the present experimental program have been carried out applying the load at the top of the column, as shown in Fig. 2a. This choice allows to directly relate the measured displacements of the joint specimen to the inter-storey drift of a whole frame (Pampanin et al., 2002). The axial load on the column is kept constant. The application of the vertical load is made through a system able to rotate along with the column, so that the load direction remains parallel to the column axis without causing P- $\Delta$  effects. Load application was cyclic quasi static under displacement control, thus permitting an adequate correlation with stiffness and strength degradation of the specimens.

The axial (vertical) force was applied by a standard hydraulic jack located at the top of the upper column. The jack is self-balanced through four steel tie rods able to transmit the load to the bottom face of the lower column. The lower column is restrained by means of a pin connection to the reaction structure while the beam is restrained with a steel strut that acts as a pin roller restraint. In such a way the joint specimens approximately experience the stresses distribution (bending moment and shear) of a real frame structure subjected to lateral loads.

The horizontal displacements were imposed at the end of the upper column with an actuator placed at a height such that the distance from the lower hinge is exactly equal to 300 cm, which is the desired inter-storey height.

The instrumentation was made up of load cells to measure applied forces and reactions, displacement transducers (LVDTs) to measure deformations and wire transducers to record displacements. The load cells were used to measure the axial compression load applied to the column, the beam reaction (i.e., the beam shear), and the horizontal load applied by the actuator. Specifically, the deformations of the joint panel were detected through 8 LVDT transducers (N1-N8 in Fig. 2b).

Furthermore, 8 LVDTs of the same type were applied to the beam (T1-T4) and to the columns (P1-P4) near to their intersection. Finally, 2 wire transducers were arranged for the measurement of the absolute horizontal displacements at the top of the column and at the beam end. The LVDTs used to measure the deformations of the joint panel enabled the determination of its contribution to the total

drift of the specimen, as discussed in the following.

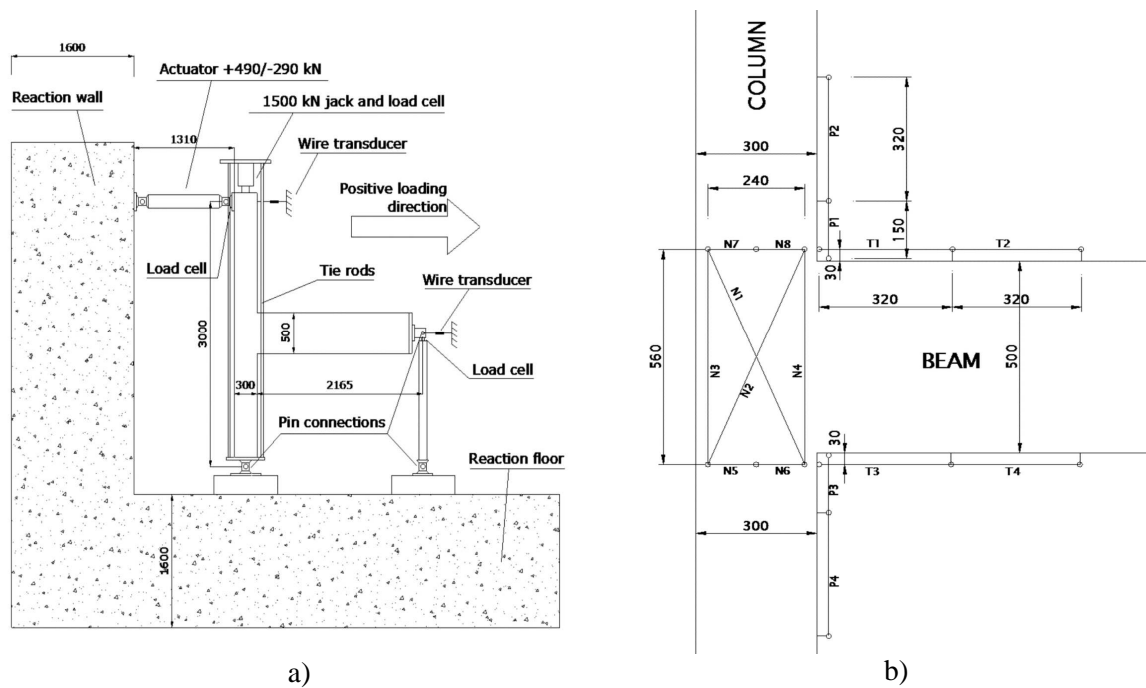


**Figure 2.** Test set-up a) and instrumentation arrangement b)

During the tests, three cycles for each drift amplitude were performed, similarly to other experimental campaigns (e.g., Braga et al. 2001), so that the possible strength degradation under repeated tests with constant amplitude can be evaluated. Once three cycles were made, the drift amplitude was increased until observing a state either of severe damage or of near collapse.

The choice of the drift values has been made taking into consideration expected (nominal) drift values at cracking and at yielding, which are around 1.0%. For this reason, the drift increasing step was smaller until drift values equal to 1.5% (a step of 0.25% was chosen), and larger (0.5%) when the drift exceeded 1.5%. In such a way it was possible to adequately follow cracking and yielding phenomena which occurred during the tests. It has to be noted that a drift limit equal to 0.5% is considered when verifying the damage limitation in RC buildings having non-structural elements of brittle materials attached to the structure (NTC08, 2008; CEN, 2004b). The maximum value of the drift was specifically decided during each test by observing the evolution of the damage conditions in order to reach a near collapse condition compatible with the safety conditions of the entire test apparatus. The rate of application of the displacement was constant and equal to 4 mm/s.

### 3. TEST RESULTS AND DISCUSSION

In this section the main results in terms of ultimate capacity and deformation behaviour found on the specimens under examination are reported and discussed. Different performances due to the amount of the axial load are analysed on the basis of the shear-drift envelopes and of the observed damage mechanisms. Further, the variation of the joint stiffness under increasing drift and the contribution of the joint-panel deformability to total deformability of the joint have been analysed.

#### 3.1. Damage mechanisms

In Fig. 3 a picture displaying the damage state at the end of each test is reported. As can be seen, very different damage patterns can be recognized for the three joints.

In specimen J5, tested under 5% of the ultimate axial compression load (i.e. 96 kN), damage affected prevalently the joint panel with a series of diagonal cracks and the spalling of the concrete cover in

the rear face of the column, probably because of the pushing effect of the beam reinforcing bars. A very small sub-vertical crack was detected at the beam-column interface, whose size did not increase while increasing the drift. Also, the faces of the joint panel were affected by an extensive spalling of concrete discovering the hoops placed in the joint core. The first cracks in the joint panel were observed when the drift reached a value approximately equal to 1.75%. However, the presence of damage at earlier stages, for example in the inner part of the joint panel, cannot be excluded.

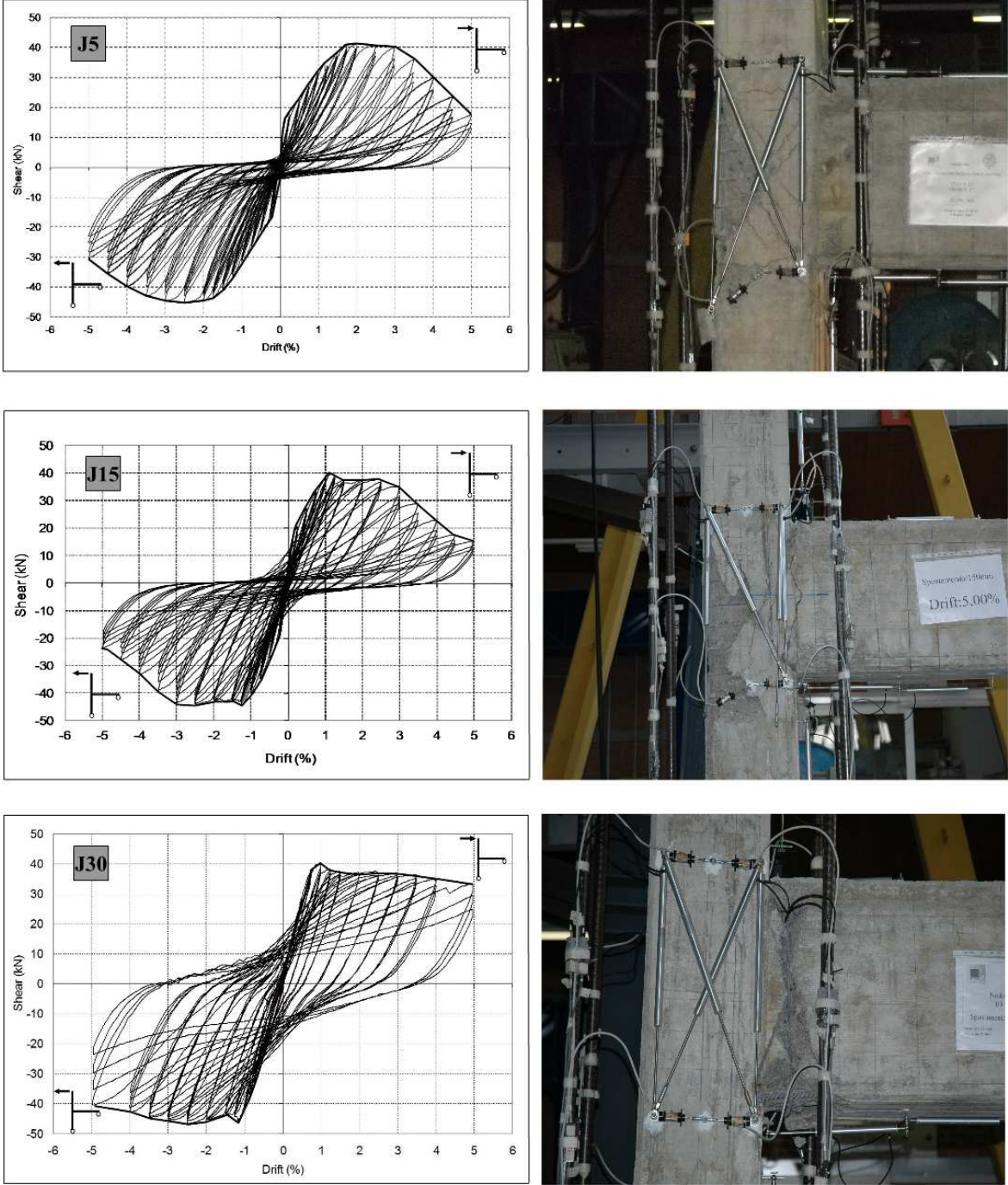


**Figure 3.** Shear-drift behaviour and final damage states

Specimen J15, tested under a larger value of the axial load (15% of the ultimate value, i.e. 290 kN), showed a damage pattern similar to that observed in joint J5, plus an additional large cracking at the beam-column interface. The latter damage was firstly detected with drift values around 0.75%. First diagonal cracks in the joint panel were detected at a drift value equal to 2.5%, higher than that found

in joint J5 (i.e. 1.75%). This result can be ascribed to the higher value of the axial load that provided a larger confining effect to the joint panel.

Specimen J30, tested under a value of the axial load equal to 30% of the ultimate value (i.e. 580 kN), exhibited a damage pattern made up of sub-vertical flexural cracks concentrated at the beam-column interface. The first cracks were observed at drift values around 0.75%. Collapse was reached because of the failure of bottom beam rebars. This unexpected result was caused by buckling effects on beam rebars that, resulting in strain concentration, led the rebars to oligocyclic fatigue failure.

It is worth pointing out that no damage has been observed in the columns of all tested specimens. This result was expected comparing the flexural strength values of columns and beam.

### 3.2. Shear-drift behaviour

Shear-drift envelopes in Fig. 3 clearly show the different hysteretic behaviour of joint J30 with respect to the other joints. In fact, Joint J30 exhibits a less degrading behaviour, thus dissipating a larger amount of energy mostly due to the plastic deformation of beam rebars. Comparing joints J5 and J15, hysteresis cycles with smaller width are found in the former one. As a consequence, it can be stated that, for the joints under study, the larger is the axial load the larger is the dissipated energy.

Further evidence of the role of axial load on the shear-drift behaviour can be found with regard to the different strength drop. Joint J30 has a small strength drop after the peak shear value. With drift equal to 5%, J30 lost about 20% of its strength, while at the same drift value joints J5 and J15 lost about 60% of their maximum strength. As a consequence, the plateau in the shear drift envelopes of the joints tested under smaller values of the axial load (J5 and J15) is shorter, leading to lower deformation capacities.

In Tab. 1 the yielding and the ultimate deformation capacities in terms of drift values  $D_y$  and  $D_u$ , respectively, are reported for what concerns the positive loading direction, i.e. the positive quadrant of shear-drift relationships in Fig. 3. The ultimate value is determined according to Panagiotakos and Fardis (2001) that proposed to conventionally establish the ultimate value of the chord rotation as the value at which the strength shows a 20% drop. The ductility values  $\mu = D_u/D_y$  clearly show how the axial load value (i.e. the only difference between the tests) can strongly influence the seismic performances of sub-assemblages like those here examined.

It is worth specifying that the above results are mainly due to the joint panel damage related to the considered axial load values, then larger values can determine different effects.

**Table 1.** Strength and deformation capacities of specimens

Joint	$F_y$ (kN)	$D_y$	$D_u$	$\mu$
J5	41.19	1.75%	3.5%	2.00
J15	39.28	1.25%	3.25%	2.60
J30	39.50	1.00%	4.96%	4.96

### 3.3. Variation of joint stiffness

In the following Fig. 4, the shear drift envelope curves are plotted. The curves are based on the shear values (obtained from the first cycle) at increasing drift amplitudes. As it can be noted, joints J5 and J15 show a small although evident variation of the curve at very low drift values, say around 0.25%. Joint J30, instead, shows a substantially linear trend of the curve until reaching drift values around 0.5%, with a slight variation beyond this value.

As a consequence, different values of drift at which the full yielding is attained,  $D_y$ , are shown by the specimens:  $D_y$  increases with decreasing axial load values. Small differences have been found when changing displacement direction, as shown in Tab. 2 where  $F_y$  values and corresponding drift values  $D_y$ , in both positive and negative quadrants, are reported.

Joint J5 reaches the full yielding at a drift value about 70% larger than that of joint J30, while joint J15 shows not so large difference with respect to joint J30. As a consequence, considering the values relevant to the positive quadrant, joint J30 has a secant stiffness  $K_{sec}$  at the shear  $F_y$  about 67% higher than that of joint J5, and nearly 30% higher than joint J15.

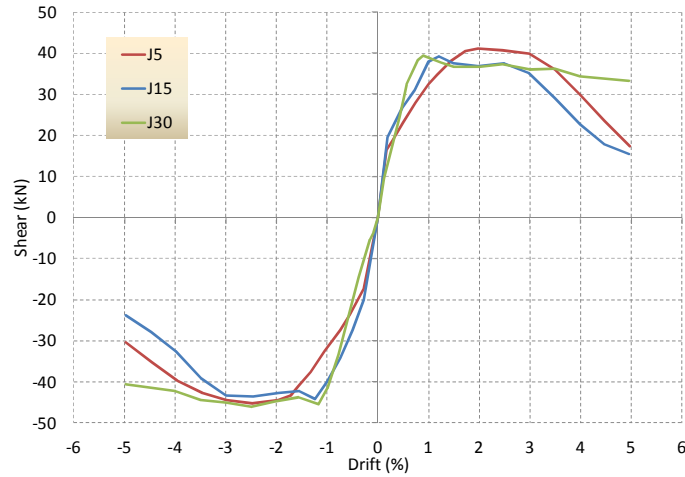


**Figure 4.** Shear-drift envelope curves

**Table 2.** Drift and secant stiffness values at the full yielding

Joint	Negative quadrant			Positive quadrant		
	$F_y$ (kN)	$D_y$ (%)	$K_{sec}$ (kN/mm)	$F_y$ (kN)	$D_y$ (%)	$K_{sec}$ (kN/mm)
J5	-45.16	-1.75	0.86	41.19	1.75	0.78
J15	-44.24	-1.24	1.19	39.28	1.25	1.04
J30	-45.50	-1.18	1.29	39.50	1.00	1.31

It is worth remembering that the only difference between the test on joints J5, J15 and J30 is the axial load value, therefore detected stiffness variations are to be ascribed to axial load variations.

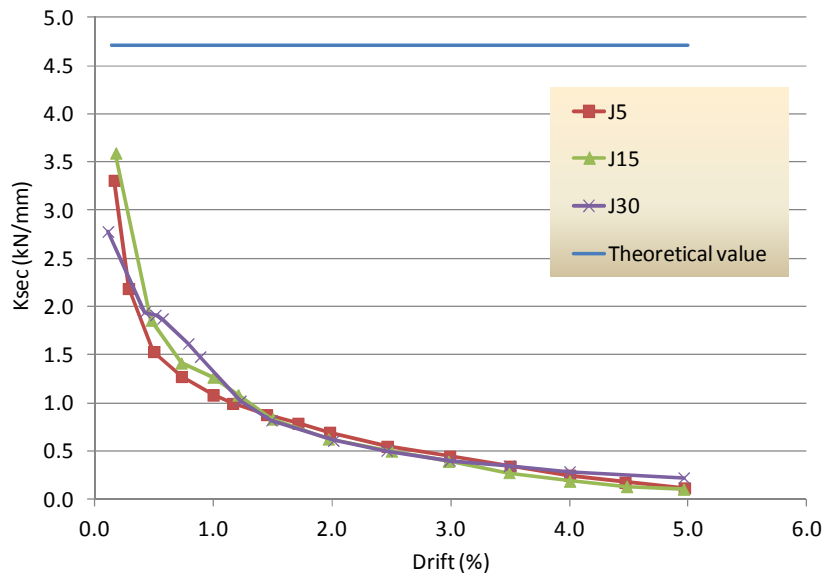


**Figure 5.** Secant stiffness-drift envelope curves

In Fig. 5 the secant stiffness values (positive quadrant) with increasing drift is plotted. As can be seen, significant differences between the examined joints can be found for drift values up to 1-1.5%. Besides, a line representing the theoretical elastic stiffness of the joint is reported in blue. This stiffness value is calculated on a linear model (the same for the three joints being the axial force not accounted for) of the joint considering a concrete having a Young modulus equal to

$$E_{cm} = 22000 \cdot \left[ \frac{f_{cm}}{10} \right]^{0.3}, \text{ where } f_{cm} \text{ is the mean cylinder strength assumed equal to 21.5 MPa.}$$

As can be noted, the theoretical value is higher than the experimental values also for very low values of drift, i.e. when cracking effects should be negligible. For drift values in the range 0.5-1.0% the theoretical secant stiffness is about 3-4 times higher than the experimental one.

### 3.4. Joint panel deformations

In order to determine the causes of the larger deformability measured under the lower values of the axial force acting on the column (as pointed out at section 3.3), the local deformations of the joint panel have been calculated through the measurements of the LVTDs placed on it. As can be seen from Fig. 2b, diagonal displacement transducers (named N1 and N2) are placed on the joint panel.

Damage occurred at the joint panel of specimens J5 and J15 did not allow to record their measurement up to the maximum drift values applied during the tests. Indeed, for high drift values, some LVDTs were removed because of concrete cover spalling. For this reason, the joint panel deformations measured on the three specimens are plotted (Fig. 6) and analysed for drift values up to 3.0%.

As can be seen, for low drift values (i.e. around 0.5%), joint panel deformations in the specimen J15 and J30 are nearly coincident (0.12% and 0.15%, respectively), while joint panel of J5 already shows a larger deformation value (0.23%). When the total drift increases the gap between J15 and J30 increases too, as well as the gap between J5 and J15, therefore it clearly brings out that the lower is the axial load the larger are the joint panel deformations, particularly for increasing drift values. On the contrary, test results on joint J30 show that local deformations in the joint panel are very low and insensitive to drift increments because damage affected only the beam at the column interface. In joints J5 and J15, joint panel deformation values ( $D_{JP}$ ) increase more than linearly with the drift.

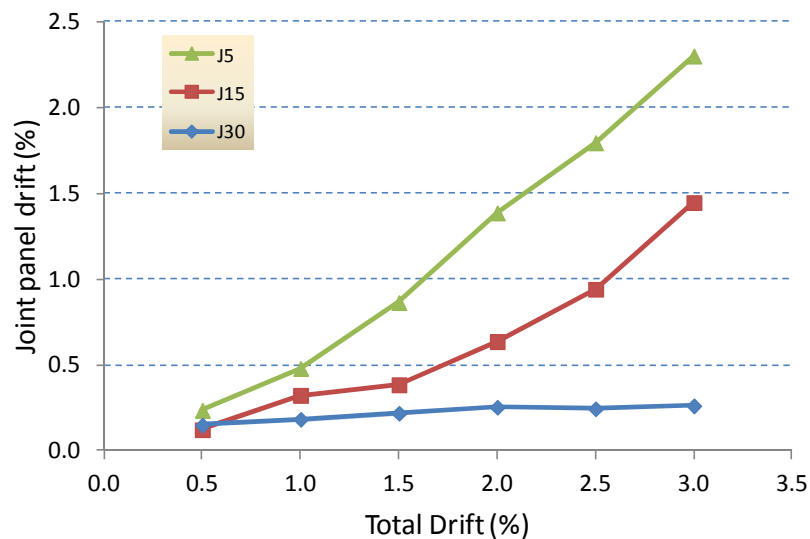


**Figure 6.** Total drift-joint panel drift envelope curves

It is interesting to analyse the contribution of  $D_{JP}$  to the total joint drift  $D$ . Tab. 3 reports the ratios  $D_{JP}/D$  (in percentage) at increasing  $D$  values. As it could be noted from the previous Fig. 6, for the joint tested under the lower axial load value (i.e. J5) most of the drift is due to the joint panel deformation: at a total drift of 3.0%, the joint panel provides 76.7% of  $D$ , with  $D_{JP}/D$  values always higher than 47%. For specimen J15, joint panel contribution to drift gets up to a maximum value equal to nearly 50%, while specimen J30 shows lower values with decreasing trend at increasing  $D$  values and, moreover, they are around 10% at the higher  $D$  values. Summing up, it is clear that beam-column joint panel can be the principal source of deformability in RC framed structures depending on the value of the axial load applied to the column and, as a result, to the collapse mechanism of the joint.

A further proof of this result can be found analysing the beam end deformation provided by the LVDT

with label T3 (see Fig. 2b), that measures the deformations at the bottom face of the beam near to the column interface (LVDT length equal to 320 mm).

**Table 3.** Contribution of joint panel deformation  $D_{JP}$  to the total drift  $D$

Total Drift (%)	J5		J15		J30	
	$D_{JP}$ (%)	$D_{JP}/D$ (%)	$D_{JP}$ (%)	$D_{JP}/D$ (%)	$D_{JP}$ (%)	$D_{JP}/D$ (%)
0.5	0.24	47.1%	0.12	24.4%	0.15	29.6%
1.0	0.48	47.9%	0.32	32.3%	0.18	18.3%
1.5	0.86	57.5%	0.38	25.6%	0.22	14.5%
2.0	1.39	69.3%	0.64	31.8%	0.25	12.6%
2.5	1.80	71.8%	0.94	37.7%	0.24	9.8%
3.0	2.30	76.7%	1.45	48.2%	0.26	8.7%

The elongation measured by T3 divided by the height of the beam provides the mean rotation of the beam due to flexure deformation in the potential plastic hinge zone.

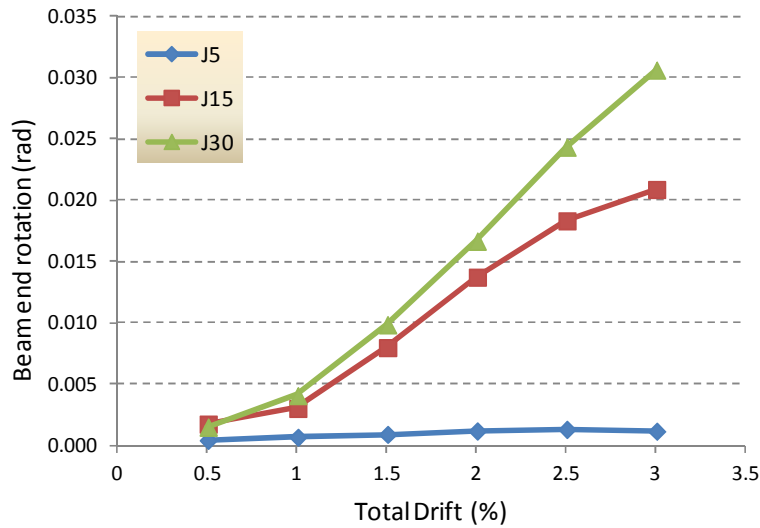


**Figure 7.** Beam end rotation at increasing total drift values

Results are plotted in Fig. 7 that shows how the beam end rotation of joint J5 is almost negligible ranging from 0.001 to 0.0012 rad, while in joints J15 and J30 there are higher values of the beam end rotation. These results are coherent with the damage observed in the joints during and at the end of the tests. Actually, joint J5 showed no significant damage at the beam-column interface, contrarily to joints J15 and, particularly, joint J30.

The present analysis confirms that also for seismic code-complying joints, as in this case, heavy damage can affect the joint panel, reducing significantly the ductility demand in the adjacent framing members, similarly to what found by Calvi et al. (2002) for gravity load designed joints. This damage mechanism appears to be directly dependent on the axial compression load acting on the columns.

#### 4. FINAL REMARKS

The paper reports and analyses some results of a wide experimental program carried out on beam-column RC joints relevant to structures with earthquake resistant design. Main objective of the paper is analysing how the axial load value on the columns can affect both ultimate capacity and stiffness of joints. To this purpose, cyclic tests have been performed on three identical specimens but varying the axial load level.

Results have shown how the value of the axial load can influence the joint behaviour in terms of both

ductile and energy dissipation capacity. Deformation capacity found in the joint tested under the larger value of axial load (J30) is more than twice that of joints with lower axial loads (J5, J15). In fact, in presence of a lower axial load, damage shifts partially (joint J15) or totally (joint J5) from the beam-column interface to the joint panel resulting in a severe cracking. However, it is worth noting that although joint panel damage occurred in joints J5 and J15, the presence of hoops into the panel did not allow instability in supporting the axial load.

According to the observed damage pattern, analysis of joint panel deformation and of beam end rotation confirmed that under low axial load the contribution of joint panel deformation to the total joint drift remarkably increases. Particularly, in joint J5 this contribution increases up to about 75% of the total drift. This effect, in turn, has repercussions on the secant stiffness of the joint as a whole. In fact, significant differences in the stiffness values have been found among the three specimens. Joint J30 shows a higher stiffness at the yielding shear, until 70% larger than the value of joint J5. By examining secant stiffness trend at increasing total drift values in J30, no significant variations can be found except in the drift range 0.5%-1.0%.

Finally, it should be considered that due to the overturning effects caused by lateral loads, the axial load on the columns can experience significant variation during a seismic event. Considering the results provided by the tests at variable axial load levels, this variation could have some influence on the beam-column performances.

## REFERENCES

- Braga, F., De Carlo, G., Corrado, G.F., Gigliotti, R., Laterza, M., Nigro, D. (2001). Meccanismi di risposta di nodi trave-pilastro in c.a. di strutture non antisismiche. *Proc. of the 10<sup>th</sup> National Conference “L’ingegneria Sismica in Italia”, Potenza-Matera* (in Italian).
- Calvi, G.M., Magenes, G., Pampanin, S. (2002). Relevance of beam - column joint damage and collapse in RC frame assessment. *Journal of Earthquake Engineering* **Vol. 6:special Issue 1**, 75-100.
- CEN Comité Européen de Normalisation (2004a). *EN 1992-1-1:2004 Eurocode 2: Design of concrete structures - Part 1-1: General rules and rules for buildings*, 2004, Brussels.
- CEN Comité Européen de Normalisation (2004b). *EN 1998-1:2004 Eurocode 8: Design of structures for earthquake resistance—Part 1: general rules, seismic actions and rules for buildings*, December 2004, Brussels.
- Fardis, M.N. (2009). *Seismic Design, Assessment and Retrofit of Concrete Buildings – based on EN-Eurocode 8*. Springer Ed.
- Hakuto, S., Park, R., Tanaka, H. (2000). Seismic load tests on interior and exterior beam-column joints with substandard reinforcing details. *ACI Structural Journal* **Vol. 97:No. 1**.
- Hwang, S., Lee, H., Wang, K. (2004). Seismic design and detailing exterior reinforced concrete beam column joints. *13<sup>th</sup> World Conference on Earthquake Engineering, Vancouver, B.C., Canada, August 1-6, 2004*.
- Kusuhara, F., Shiohara, H. (2008). Tests of R/C beam-column joints with variant boundary conditions and irregular details on anchorage of beam bars., *14<sup>th</sup> World Conference on Earthquake Engineering, October 12-17, 2008, Beijing, China*.
- Masi, A., Santarsiero, G., Nigro, D. (2012). Cyclic Tests on External RC Beam-Column Joints: Role of Seismic Design Level and Axial Load Value on the Ultimate Capacity, *Journal of Earthquake Engineering*  
DOI: 10.1080/13632469.2012.707345  
(Published on line on July 06 2012, <http://www.tandfonline.com/doi/abs/10.1080/13632469.2012.707345>).
- NTC08 D.M. 14 gennaio 2008 Ministero delle Infrastrutture. (2008). *Norme tecniche per le costruzioni* (in Italian). Available at <http://www.cslp.it>
- Pampanin, S., Calvi, G.M., Moratti, M. (2002). Seismic behaviour of R.C. beam-column joints designed for gravity loads. *12<sup>th</sup> European Conference on Earthquake Engineering, EAEE, London*.
- Panagiotakos, T.B., Fardis, M.N. (2001). Deformation of reinforced concrete members at yielding and ultimate. *ACI Structural Journal* **Volume 98:No. 2**, 135-148.
- Park, R., (2002). Summary of results of simulated seismic load tests on reinforced concrete beam-column joints, beam and column with substandard reinforcing details. *Journal of Earthquake Engineering* **Vol. 6:No.2**, 147-174.
- PCM Presidenza del Consiglio dei Ministri. (2003). OPCM 3274 e s.m.i. - Allegato 2 Norme tecniche per il progetto, la valutazione e l’adeguamento sismico degli edifici. G.U. 8/5/2003 (in Italian).
- Paulay, T., Priestley, M. J. N. (1992). *Seismic design of reinforced concrete and masonry buildings*. John Wiley & Sons, New York.